

The elastic scattering of ${}^6\text{Li}+{}^{28}\text{Si}$ at near-barrier energies

A. Pakou^a, N. Alamanos^b, A. Lagoyannis^a, A. Gillibert^b,
E. C. Pollacco^b, P. A. Assimakopoulos^a, G. Doukelis^c,
K. Ioannides^a, D. Karadimos^a, D. Karamanis^a, M. Kokkoris^c,
E. Kossionides^c, N. G. Nicolis^a, C. Papachristodoulou^a,
N. Patronis^a, G. Perdikakis^c, D. Pierroutsakou^d

^a*Department of Physics, University of Ioannina, 45110 Ioannina, Greece*

^b*CEA-Saclay, DAPNIA-SPhN, Gif-sur-Yvette, France*

^c*National Research Center Demokritos-Greece*

^d*INFN Sezione di Napoli, I-80125, Napoli, Italy*

Abstract

The ${}^6\text{Li}+{}^{28}\text{Si}$ elastic scattering was studied at near-barrier energies with the aim to probe the threshold anomaly. Angular distributions were measured over a wide angular range ($\theta_{lab}=25^0$ to 150^0) at 4 energies, namely 7.5, 9, 11 and 13 MeV. The present data together with previous ones at higher energies, as well as elastic scattering data of ${}^6\text{Li}$ on various targets at near barrier energies, were analyzed by using optical potentials obtained in a double-folding framework. It was found that the strength of the real part of the potential remains almost independent of energy down to, and possible even below, barrier, while the strength of the imaginary part presents an increase at near barrier energies. The results are discussed.

Key words:

elastic scattering ${}^{28}\text{Si}({}^6\text{Li}, {}^6\text{Li})$, measured $\sigma(\theta)$, double-folding potentials, deduced optical model parameters, threshold anomaly, weakly bound nuclei, sub-barrier fusion.

PACS: 25.70.Bc, 24.10.Ht, 27.20.+n

When studying elastic scattering between two stable ions at energies well above the Coulomb barrier, it is adequate to ignore specific effects due to couplings to other reaction channels. It is then plausible to describe scattering by phenomenological or folding potentials which vary slowly with energy. This picture no longer remains valid when approaching the vicinity of the

Coulomb barrier. Couplings between various channels increase in importance and in describing elastic scattering, either these couplings have to be taken into account through coupled channel theories, or the energy dependence of the various optical model parameters has to be considered explicitly. In fact, the term "threshold anomaly" was invoked to describe a rapid variation of such model parameters around the barrier. This variation is visualized as a localized peak in the strength of the real potential, associated with a sharp decrease in the strength of the imaginary potential as it becomes more and more unimportant to remove flux from the reaction in this low energy region. The significance of this phenomenon, revealed by elastic scattering data, is demonstrated in the interpretation of data in other reaction channels. In that respect, near- and sub-barrier fusion cross sections for stable nuclei have been reproduced [1,2] by using a barrier penetration model with an energy dependent potential corresponding to the threshold anomaly.

Moving to weakly bound nuclei the situation becomes more complicated due to the influence of breakup effects. It is believed that the polarization potential which is produced by the break up, as it is repulsive in nature, will compensate the attractive term of the potential ΔV ($V=V_0+\Delta V$) which is connected through a dispersion relation with the imaginary part and which is responsible for the anomaly. Otherwise, as it is suggested by Satchler [3], the dispersion relation may be of no use for weakly bound systems, since according to theoretical calculations [4], the repulsive contribution of the real part of the potential, is almost independent of beam energy while the associated imaginary potential is very small.

The study of ${}^6\text{Li}$ on various stable systems was undertaken by several authors in the past [5–10] and in recent years the emphasis was on the threshold anomaly [10,5]. The trend of such studies pointed out to a energy independent real potential, which was interpreted as the result of an absence of the anomaly for weakly bound systems. However, this result was supported by data, most of them determined at energies well above the Coulomb barrier and only few of them near the barrier. Near the barrier, departures from Rutherford scattering are mostly featureless, and thus more data are necessary, and in preference with light targets where the Coulomb potential is smaller, in order to draw a strong statement.

To contribute in that direction, we have undertaken the study of the ${}^6\text{Li}+{}^{28}\text{Si}$ elastic scattering at near-barrier energies. It should be noted that the lowest energy this system was studied before was at 13 MeV, while the Coulomb barrier in the laboratory is at 8.5 MeV [11].

A ${}^6\text{Li}^{+2}$ beam was delivered by the TN11/25 HVEC 5.5 MV Tandem accelerator of the National Research Center of Greece-DEMOKRITOS at four bombarding energies, namely 7.5, 9, 11 and 13 MeV. Beam currents were of

the order of 30 nA. The beam impinged on a 180 μm thick, self supported natural silicon target tilted by $\pm 40^\circ$ (depending on the detector position) and the elastically scattered Li ions were detected in four solid state surface barrier detectors. Two of these detectors were telescopes (the ΔE silicon detector was 10 μm thick while the E detector was 300 μm thick) and measured the forward-angle scattering while the other two were thin, 20 or 25 μm thick silicon detectors and measured the backward scattering. The choice of the thickness of the backward detectors was such as to allow, light particles like alpha's from breakup transfer and other contaminant reactions (${}^6\text{Li}+{}^{12}\text{C}$) to go through while, Li particles to stop in the detectors. The alpha group was well discriminated in the forward detectors with the ΔE -E technique. The detectors were set 30 cm far from the target on a remote control rotating table, two of them upstream and two downstream of the target to compensate for non-centrality beam problems. Tantalum masks were placed in front of each telescope and each detector and an angular resolution of 0.7° was obtained. This angular uncertainty was estimated to be 2° due to the beam divergence. The subtending solid angle was 1.2×10^{-4} sr. An overall normalization was obtained at each energy by placing two monitor Si(Li) detectors, 300 μm thick, at $\pm 15^\circ$, fixed on a top table concentric to the bottom rotating one. The scattering at 15° , concerning the present bombarding energies, can be considered as being pure Rutherford. A liquid - nitrogen cold trap close to the target holder, reduced the target contamination on carbon to minimum. This was confirmed at the end of the runs in a separate RBS (Rutherford Back Scattering) experiment [12] during which the carbon contaminant was estimated and the target thickness was established.

Angular distributions were determined in steps of 2 to 10 degrees depending on energy. The data were recorded in the PC controlled acquisition system, CAMDA [13] and were analyzed off line. The results are shown in Fig. 1. Former results obtained at 13 MeV [6] are also plotted and they present an excellent consistency with our data.

For the theoretical analysis, elastic scattering calculations were performed with the code ECIS [14]. The real part of the entrance potential was calculated within the double folding model [15] by using the BDM3Y1 interaction developed by Khoa et al. [16]. This interaction has been found before [17,18] to describe rather well elastic scattering data at high energies for both stable and weakly bound nuclei, as long as the normalization factor for the weakly bound ones was substantially reduced due to breakup effects. In fact, data for ${}^6,7\text{Li}$ and ${}^9\text{Be}$ nuclei on various targets [5,10,15,17,19,20], required a renormalization of the real folded potential by a factor of $N \sim 0.6$ for energies well above the Coulomb barrier.

The densities involved in the real double folded potential of the present analysis, were obtained from electron scattering data, adopting a standard pro-

cedure - a three parameter Fermi model, for ^{28}Si [21], while following the phenomenological relation adopted by Bray et al. [22] for ^6Li .

For the imaginary part we considered two different types of potentials. Initially we adopted a Woods-Saxon potential and we performed a grid search taking as a free parameter the normalization factor N , of the real potential, while stepping the three parameters of the Woods-Saxon imaginary one, till the best fit was obtained. A second fit was also obtained with only two free parameters, the normalization factor N of the real part of the potential and the depth W of the imaginary one at a fixed radius and diffuseness. The χ^2 obtained in that fit was very close to the one of the best fit. The results are shown in Table I.

Subsequently, the imaginary potential was assumed to be of the same radial shape as the real one, and the same folded potential was adopted but with different normalization factor. A search was performed with free parameters the two normalization factors for the real and imaginary potential, N_R and N_I . The results of the best fits are shown in Table II, while the deduced angular distributions are compared with the data in Fig. 1. Former data at 20, 27 and 34 MeV were also fitted and the results concerning the optical model parameters are given in Tables I and II, while the calculated angular distributions in Fig. 1. A first inspection of Fig.1 shows that at 7.5 MeV we are already well below the barrier and almost all the scattering is Rutherford. For that reason, fits to these data were omitted being very insensitive to the nuclear potential.

From Tables I and II and from Fig. 2, where the real and imaginary normalization factors are plotted as a function of the lithium bombarding energy, we can draw the following conclusions. The results are consistent with an optical potential where the normalization factor for the real part, for energies both near and well above the barrier, is almost independent of energy. On the other hand the imaginary part presents an increasing behaviour (well depth for the Woods-Saxon potential-Table I, normalization factor N_I for the folded potential-Table II, Fig. 2) around the barrier in accordance with the trend which was noticed before by Keeley et al. [5] for the $^6\text{Li}+^{208}\text{Pb}$ system, but without to exclude a more constant behaviour [10], due to the big uncertainties quoted in both works. To fully clarify this interesting point we performed systematically elastic scattering calculations in our folding potential framework for the following systems: $^6\text{Li}+^{58}\text{Ni}$, $^6\text{Li}+^{118}\text{Sn}$ and $^6\text{Li}+^{208}\text{Pb}$, where data exist at near barrier bombarding energies [23,5]. The results, concerning the behaviour of the real and imaginary part of the potential, are presented in Fig. 3 as a function of the ratio of the bombarding energy over the BDM3Y1 potential barrier which was deduced from our calculations. The adopted errors, 10% to 20% and 20% to 40% for the real and imaginary potential respectively, were deduced from a sensitivity analysis performed by varying the parameters, N_R and N_I , by certain amounts.

A striking difference between the real and the imaginary part is now revealed. While the strength of the real part of the potential remains constant, almost independent of energy down to, and possible below, barrier the strength of the imaginary part presents a well developed increase around the barrier. Such a behaviour is beyond doubt contradictory with the one met on stable projectiles and expressed via the threshold anomaly. It leads to the following conclusions. To start with, the reduction of the normalization factor of the real part of the potential for the higher energies to $N \sim 0.6$ is well understood, as already was discussed in the introduction, and is due to the development of a repulsive polarization potential produced by breakup. The fact that the same reduction persists even at energies around the coulomb barrier may indicate either an energy dependence of the breakup polarization potential in the presence of the anomaly (the polarization potential becomes more repulsive and compensates the attractive term of the real potential-the anomaly), or an almost constant polarization potential in the absence of the anomaly. The first suggestion is corroborated by the increase of the imaginary part around the barrier. Such an increase is predicted by theoretical calculations and it is attributed either to transfer reactions [26] as in the case of ${}^7\text{Li}+{}^{208}\text{Pb}$ or to break up produced in the coulomb field which becomes important at these energies [27]. Moreover this picture is also supported by experimental measurements of breakup/transfer cross sections around the barrier, which almost exhaust the total reaction cross section, $\sigma_{break/transfer} \sim 0.70\sigma_{tot}$ [23,25,28]. In that case, this "additional" break-up or/and transfer, is responsible for the energy dependence of the real polarization potential which becomes more repulsive around the barrier and compensates the attractive term (increase of the real potential) seen in the threshold anomaly. Explicit calculations using dispersion relations between real and imaginary parts, in the presence of a strong break-up channel, are necessary to disentangle this point. A similar increase on the imaginary part of the potential, noted in the study of Aguilera et al. [24] for the system ${}^6\text{He}+{}^{209}\text{Bi}$ shows the significance of the present result on the consequences upon halo nuclei potentials and the interpretation of reaction channels where they are involved.

Summarizing, the elastic scattering of ${}^6\text{Li}+{}^{28}\text{Si}$ was measured at near barrier energies. The present data, as well as previous data at higher energies and elastic scattering data of ${}^6\text{Li}$ on various targets, were considered and analysed systematically in the same folding framework. It was found that the strength of the real part of the potential remains independent of energy down to, and possible below, barrier while the strength of the imaginary part presents an increase around the barrier. This behaviour is contradictory to the one exhibited by stable projectiles described as threshold anomaly. Within the present work, it is suggested that the influence of an additional strong breakup and/or transfer channel developed around the barrier, produces a more repulsive polarization potential in this energy region which compensates the attractive part of the real potential. However, more elaborate calculations using explicitly dis-

persion relations between the real and the imaginary part of the potential, are necessary to pin down the type of the anomaly for weakly bound systems. This will give also an interesting insight in the behaviour of the potential of halo nuclei with consequences in the interpretation of data in various reaction channels.

Acknowledgements

We would like to warmly aknowledge Mr John P. Greene from the Argonne National Laboratory, for providing the silicon targets and Dr K. Rusek and F. Auger for useful discussions. One of us (Athena Pakou) would like to aknowledge a partial finacial support approved by the Rector of the University of Ioannina, Prof. Christos Massalas.

References

- [1] G.R. Satchler, Phys. Reports 199 (1991) 147.
- [2] M. A. Nagarajan and G.R. Satchler, Phys. Lett. B 173 (1986) 29.
- [3] C. Mahaux, H. Ngo, G.R. Satchler, Nucl. Phys. A449 (1986) 354.
- [4] Y. Sakuragi et al. Prog. Theor. Phys. 68 (1982) 322;70 (1983) 525.
- [5] N. Keeley et al., Nucl. Phys. A571 (1994) 326.
- [6] J.E. Poling, E. Norbeck, R.R. Carlson, Phys. Rev. C 13 (1976) 648.
- [7] J. Cook, Nucl. Phys. A375 (1982)238.
- [8] M.F. Vineyard, J. Cook, K.W. Kemper, Nucl. Phys. A405 (1983) 429.
- [9] R.I. Cutler, M.J. Nadworny and K.W. Kemper, Phys. Rev C15 (1977) 1318.
- [10] M. A. Tiede, D. E.Trcka and K.W.Kemper, Phys. Rev. C 44 (1991) 1698.
- [11] Ricardo. A. Broglia and Aage. Winther, Heavy Ion Reactions, Volume I: Elastic and Inelastic Reactions; The Benjamin/ Cummings Publishing Company, Inc (1981).
- [12] M. Kokkoris, private communication.
- [13] CAMDA : Camac Data Aqcuisition System, H. Steltzer, private communication, e-mail:H.Steltzer@gsi.de
- [14] J. Raynal, Phys.Rev. C 23 (1981) 2571.
- [15] G.R. Satchler and W.G. Love, Phys. Rep. 55 (1979) 183.
- [16] D.T. Khoa et al., Phys. Lett. B 342 (1995) 6.

- [17] L. Trache et al., Phys. Rev. C 61 (2000) 024612.
- [18] D.T. Khoa, G.R. Satchler, and W. von Oertzen, Phys. Rev. C 56 (1997) 954.
- [19] M.E. Brandan and G.R. Satchler, Phys. Rep 285 (1997) 143.
- [20] C.B. Fulmer et al., Nucl. Phys. A427 (1984) 545.
- [21] H.D. De Vries, C.W. Jager and C. De Vries, Atomic data and Nuclear Data Tables 14 (1974) 479 .
- [22] K.H. Bray et al., Nucl. Phys. 89 (1972) 35.
- [23] K. O. Pfeiffer, E. Speth and K. Bethge, Nucl. Phys. A206 (1973) 545.
- [24] E.F. Aguilera et al., Phys. Rev. Lett. 84 (2000) 5058.
- [25] G.R. Kelly et al., Phys. Rev. C 63 (2000) 024601.
- [26] N. Keeley and K. Rusek, Phys. Rev. C 56 (1997) 3421 ; I. Martel et al. Nucl. Phys. A582 (1995) 357.
- [27] W. G. Love, T. Terasawa, and G. R. Satchler, Nucl. Phys. A291 (1977) 183.
- [28] C. Signorini et al., Eur. Phys. Journal A 10 (2001) 249.

E_{lab} (MeV)	N_1	W (MeV)	r_0 (fm)	α (fm)	N_2	W (MeV)
9.0	0.66	32	1.20	0.57	0.58	22.1
11.0	0.62	38	1.195	0.49	0.49	20.2
13.0	0.56	28	1.16	0.74	0.67	26.2
20.0	0.69	17	1.21	0.60	0.66	16.4
27.0	0.66	17	1.21	0.63	0.66	15.9
34.0	0.62	17	1.18	0.69	0.62	15.7

Table 1

Best fit optical potential parameters. The real part of the potential was calculated in a double-folding framework with a normalization factor N (see also text). The type of the imaginary potential was assumed to be Woods-Saxon, with W , r_0 and α , the depth, the radius $R=r_0(A_1^{1/3}+A_2^{1/3})$ and the diffuseness correspondingly. N_1 corresponds to a free fit to all parameters as described in the text, while N_2 corresponds to a fit with two free parameters N and W at a fixed radius with $r_0=1.2$ fm and also a fixed diffuseness $\alpha=0.67$ fm.

E_{lab} (MeV)	N_R	N_I
9.0	0.47	0.47
11.0	0.40	0.52
13.0	0.59	0.80
20.0	0.58	0.49
27.0	0.63	0.44
34.0	0.65	0.48

Table 2

Best fit optical potential parameters. Both the real and imaginary part were assumed of the same nature and were calculated in a double-folding framework with two different normalization factors, N_R and N_I , for the real and imaginary part respectively.

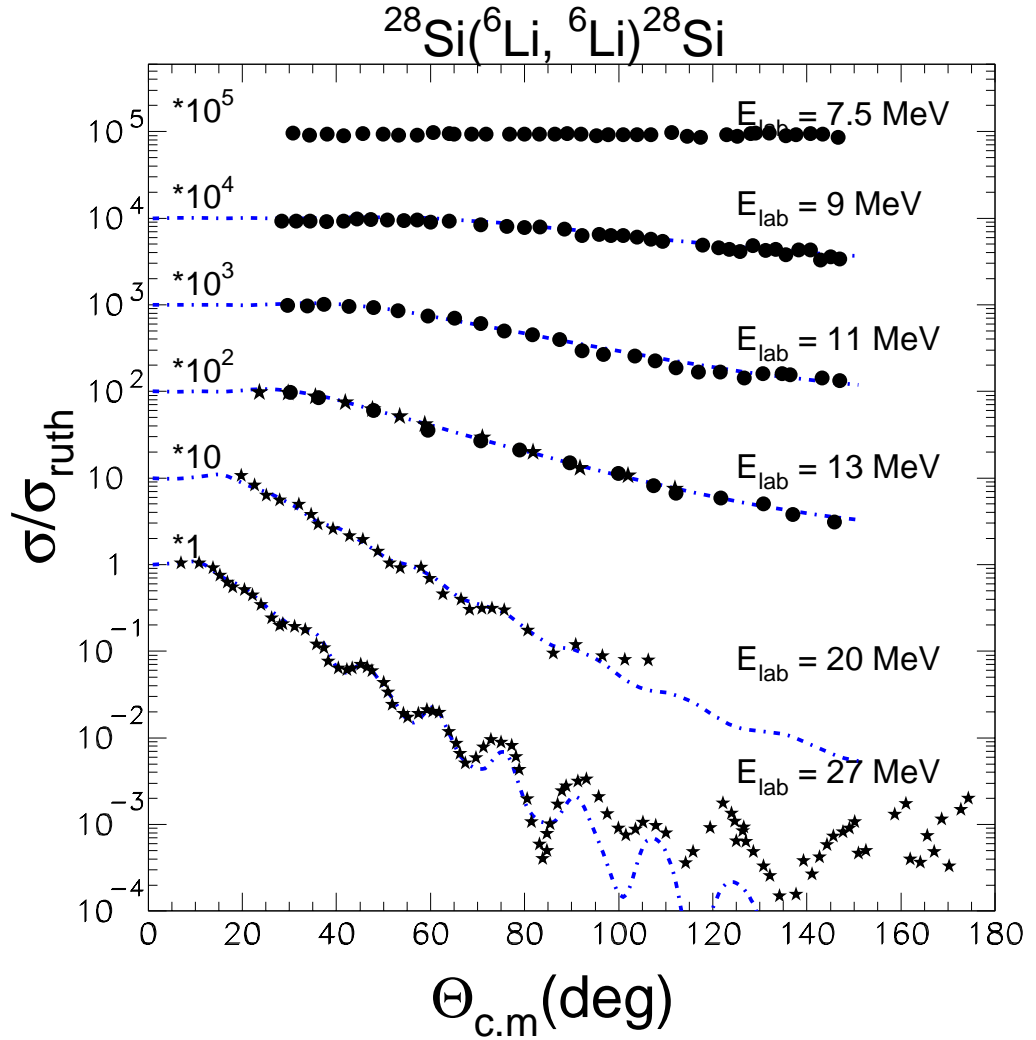


Fig. 1. New and old data for the system $^6\text{Li}+^{28}\text{Si}$. The data of the present work at 7.5, 9, 11 and 13 MeV are designated with solid circles, while the old data ([6–8]) at 13, 20 and 27 MeV with stars. The statistical error for the present data was 1 to 5 %, while the error adopted in all our fits was 10 %. The dotted dashed lines represent the best fits adopting a double folded potential for the real and imaginary part. The normalization factors are given in Table II

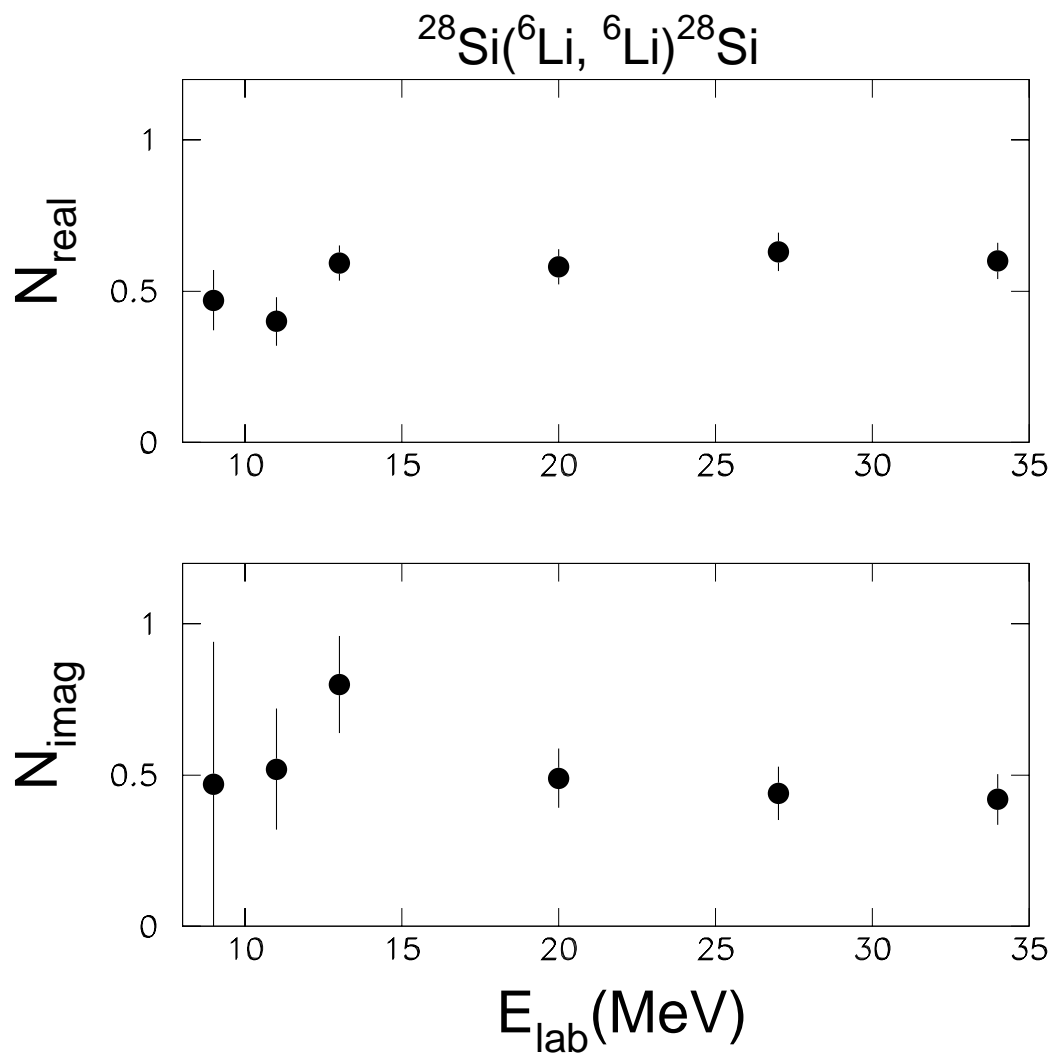


Fig. 2. Normalization factors of the real and imaginary potential for $^6\text{Li}+^{28}\text{Si}$ as a function of the lithium bombarding energy

